



ELSEVIER

Available online at www.sciencedirect.com

ScienceDirect

journal homepage: www.elsevier.com/locate/ijhydene

Electromagnetic design of a new axial and radial flux generator with the rotor back-irons

Erol Kurt ^{a,*}, Halil Gör ^b, Umut Döner ^c

^a Gazi University, Faculty of Technology, Department of Electrical and Electronics Engineering, 06500 Teknikokullar, Ankara, Turkey

^b Hakkari University, Faculty of Engineering, Department of Electrical and Electronics Engineering, 30000 Hakkari, Turkey

^c Gazi University, Institute of Science, Division of Electrical and Electronics Engineering, 06500 Teknikokullar, Ankara, Turkey

ARTICLE INFO

Article history:

Received 15 November 2015

Received in revised form

7 February 2016

Accepted 8 February 2016

Available online 4 March 2016

Keywords:

Axial flux

Generator

Back-iron

Permanent magnet

Power

ABSTRACT

The design and simulation of a new three-phase axial flux generator have been performed. The generator is a permanent magnet machine (PMG) and consists of two rotors at two sides and a stator at the middle. In the machine, each rotor has 16 rare earth disc-type magnets and back-iron units and the stator at the middle has 24 coils. It has been understood that the generator produces directly sinusoidal output and requires no conversion in the wave shape. The 3D simulations have been performed via the finite element analysis (FEA) method by the magnetostatic and magnetodynamic tools. It has been found that the machine generates 3.4 kW at 1000 rpm for the air gap of 1.5 mm. This gives the power density of 336 kW/m³ for the rated value of the generator and it is higher than the power densities of many axial flux generators in the literature. The maximal cogging torque value has been estimated as 3.6 Nm, which is a good value for a back-iron machine. It has been also proven that the waveform harmonics become lower at higher rotor speeds.

Copyright © 2016, Hydrogen Energy Publications, LLC. Published by Elsevier Ltd. All rights reserved.

Introduction

The use of rare earth elements in the production of permanent magnets (PMs) has accelerated the permanent generator production. That has enhanced the importance of permanent magnet synchronous machines (PMSM) in the wind energy market. PM generators became popular in 1980's, after NdFeB magnets were invented [1,2]. Since higher energy densities, low cogging torque value, low cost and high mechanical

torque can be available with these machines, the PM generators have been used in many applications [3,4].

According to the literature [5], PM generators have some superiorities over the asynchronous or current excited synchronous generators. Efficiency, stability and reliability comes in the first order to study on these generators [5]. They even can produce direct sinusoidal current and that is counted among the other advantages [6]. Strictly speaking, two distinct PMG structures are found in the literature: Axial flux and radial flux PMGs. If the flux goes through the coils in the radial direction, that is a radial flux generator, however if the flux

* Corresponding author.

E-mail address: ekurt52tr@yahoo.com (E. Kurt).

<http://dx.doi.org/10.1016/j.ijhydene.2016.02.034>

0360-3199/Copyright © 2016, Hydrogen Energy Publications, LLC. Published by Elsevier Ltd. All rights reserved.

passes perpendicular to the radial direction, it is an axial flux machine [7]. Indeed, the flux direction becomes parallel to the moving axis in the latter structure.

The axial flux machines become appropriate for especially medium speed applications. This reality makes them useful in moment control, machine units, robotics, electrical vehicles as well as wind energy [8]. According to the researches, they have another advantage on wind energy applications since these generators do not require an additional gear system inside the wind turbine [1,9,10]. It means that the rotation effect can be directly applied on the generator via the turbine blades. In addition, the rotor speed and power densities do not exhibit a basic correlation. There exist many studies on different types of axial generators with various power densities. Basically the power densities can have values from 6 kW/m³ to 700 kW/m³ [11].

In a previous design [6], Kurt et al. studied a radial/axial flux generator having one phase and 12 poles. In this generator, they have observed a power density of 28.5 kW/m³. However this machine was not a preliminary design of a new type core and the effect of this new core on the cogging torque has been studied compared to a bar-shaped core. It has been proven that the new core has certain advantages over the bar-shaped one in order to decrease the cogging torque values. This one phase machine has maximal output power for 5 Ω and increasing efficiency for high rotor speeds upto 1000 rpm. According to simulations, the machine has a cogging torque value of 25 mNm which is nearly the half of the bar-shaped core. Besides, the experimental output has proven that the signal type is sinusoidal and has some harmonics for lower rotor speeds as result of mechanical contact [6].

In the electromagnetic designs, the moving units of the machines, especially rotors should be mechanically durable and light. Indeed, these units are the important parts to determine the operational life of the machine, which becomes much vital for medium and high rotation speeds. However, in the case of the stator part, the magnetic flux over the stator coils and the frequency of the stator current are important [12]. All these factors may cause problem in high speeds and they can be solved by good mechanical and electromagnetic designs.

In the case of conventional axial flux PMGs, they have lower cogging torque, higher power density and efficiency, easy maintenance, lower volume and cost [9,13–17]. The machine designs still focus on lowering cogging torque, increasing the electrical power and efficiency, whereas, as an important artifact, AFPMGs have a cooling problem [18]. Indeed the cores, coils and stator units get heat due to the magnetic flux rotation inside the cores and current circulation in the windings. For instance, according to Li and his colleagues [14], high power density causes heating problems in PMGs. Therefore an appropriate mechanical design should be explored to cool down them. One way is the adjustment of air gap distance, since it assists to decrease the cogging torque, acoustic noises and mechanical vibrations [19]. Other way is the shape of the core, since it affects the cogging torque. Another solution is to decrease the losses in the machine. With that regard, Vansompel and his colleagues [10] investigated the efficiency of an axial flux machine in terms of core mass, shape and lamination. They proved that the varying air

gap can decrease the core losses within the rate of 8% and assists to improve the efficiency for continuous working conditions [20].

In the present paper, we report the results of a new designed three phase axial/radial flux machine. Mainly the new machine uses a different core shape. The coils have different winding numbers and the diameters of the rotors are certainly different. Section [Design properties of new AFPMG](#) introduces the units of the machine. The electromagnetic 3D simulations and transient solutions over flux, flux density, voltage and power are presented in Section [Magnetostatic simulations of PMG](#). Finally, the concluding remarks are given in the conclusions.

Design properties of new AFPMG

In order to produce the design and simulations, a finite element programme has been used. In the simulation environment, the definition of the simulation volume and machine units with the corresponding meshes, the material characteristics are performed to all units. [Table 1](#) presents the design parameters of new generator. The stator unit has two types of windings attached to both tips of the cores.

While one series have larger winding numbers (i.e. 300), other series have lower winding numbers (i.e. 200). However, if the serial connection is provided among the series, there exists no waveform difference between two serial connected coils. Indeed, the coils with larger sectional areas gives larger amplitude compared to the smaller one.

The air gap is adjusted as 1.5 mm for two sides of the stator located at the middle. The cross-section view of the PMG is shown in [Fig. 1](#). Two rotors are positioned on the upper and

Table 1 – Design parameters of the machine.

Components	Features
Inner radius of rotor R ₂ (mm)	75
Outer radius of rotor R ₂ (mm)	105
Inner radius of rotor R ₁ (mm)	120
Outer radius of rotor R ₁ (mm)	150
Inner radius of stator disc (mm)	70
Outer radius of stator disc (mm)	155
Thickness of back-irons (mm)	5
Radial width of back-irons (mm)	40
Coil inner diameter (mm)	30
Small coil outer diameter (mm)	46.4
Large coil outer diameter (mm)	69.6
Phase	3
Winding turns for large coil	300
Winding turns for small coil	200
Coil number	24
Wire diameter (mm)	0.75
Magnet type	NdFeB
Magnet shape	Circular
Magnet number	16
Magnet diameter (mm)	30
Magnet thickness (mm)	5
Core material	M19
Core type	Axially/radially laminated
Core number	12
Air gap (mm)	1.5

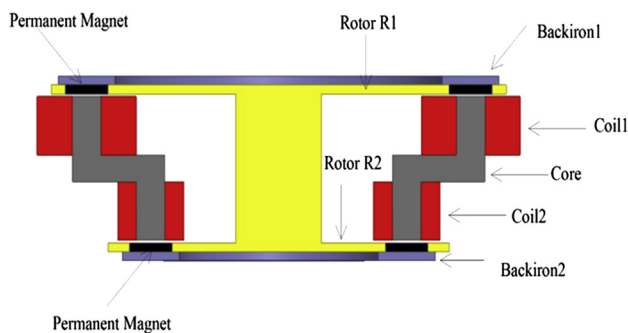


Fig. 1 – Structural design of the AFPMG.

lower sides of a stator as seen in Fig. 1. Rotor-1 which has larger coils is located top, whereas the Rotor-2 is located bottom. The cores and the location of sample magnets are also obvious in Fig. 1.

The machine stator has 24 circular coils located at the tips of 12 individual cores. The machine has 16 circular magnets in each rotor, having a good sinusoidal output. In addition, the machine has two circular back-irons located top and bottom. The powerful side of this geometry is that the cooling of the machine can be made efficiently from bottom to top, since there exists sufficient region for this purpose at the outer part of the small rotor. In a recent paper, Rasekh and his colleagues [21] have carried out a computational fluid dynamics study. They have found that the convective heat transfer reaches a minimum at a certain gap size ratio for the stator part of a disk type axial flux generator. In addition, the maximal temperature 110 °C is reached during the operation in the rotor and stator surfaces, which are high enough to make drawback to the generator. Thus, their results emphasize the importance of the geometric structure of the machine. In the present design, the cores assist to decrease the total reluctance. In addition, back irons also decrease the reluctance in that manner. The usage of the laminated cores minimizes the core losses in the machine [10]. The $B-H$ curve of the core material M19 is sketched in Fig. 2. This curve has been determined for the material in simulation. It basically gives $B = 1.4$ T flux density for the field strength $H = 1000$ A/m. This flux density is found sufficient for the maximal flux production inside the

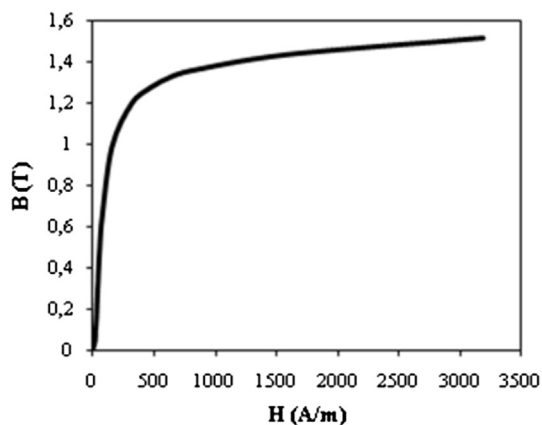
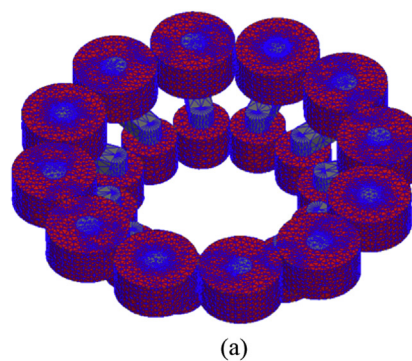
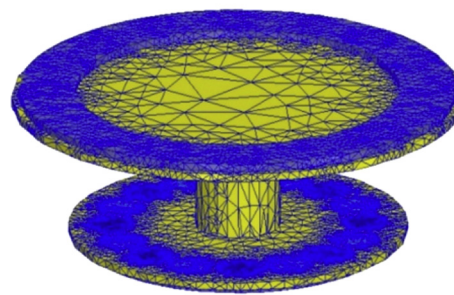


Fig. 2 – The $B-H$ curve of the core.



(a)



(b)

Fig. 3 – The meshed structures of (a) stator and (b) rotor units.

core. The same material has also been used for back-iron units.

For the finite element analyzes, the meshed forms of stator and rotors are shown in Fig. 3(a,b). While 237326 mesh cells are used in the stator unit, 156148 mesh cells are found sufficient for the rotor units. An optimized number of cells have been obtained by comparing the experimental value of voltage. Indeed, the increase in the mesh numbers is a

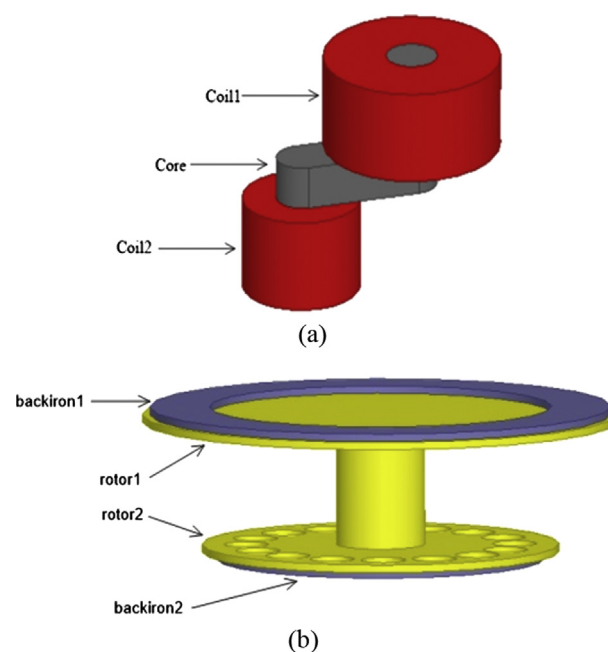


Fig. 4 – The design of (a) core and (b) back irons.

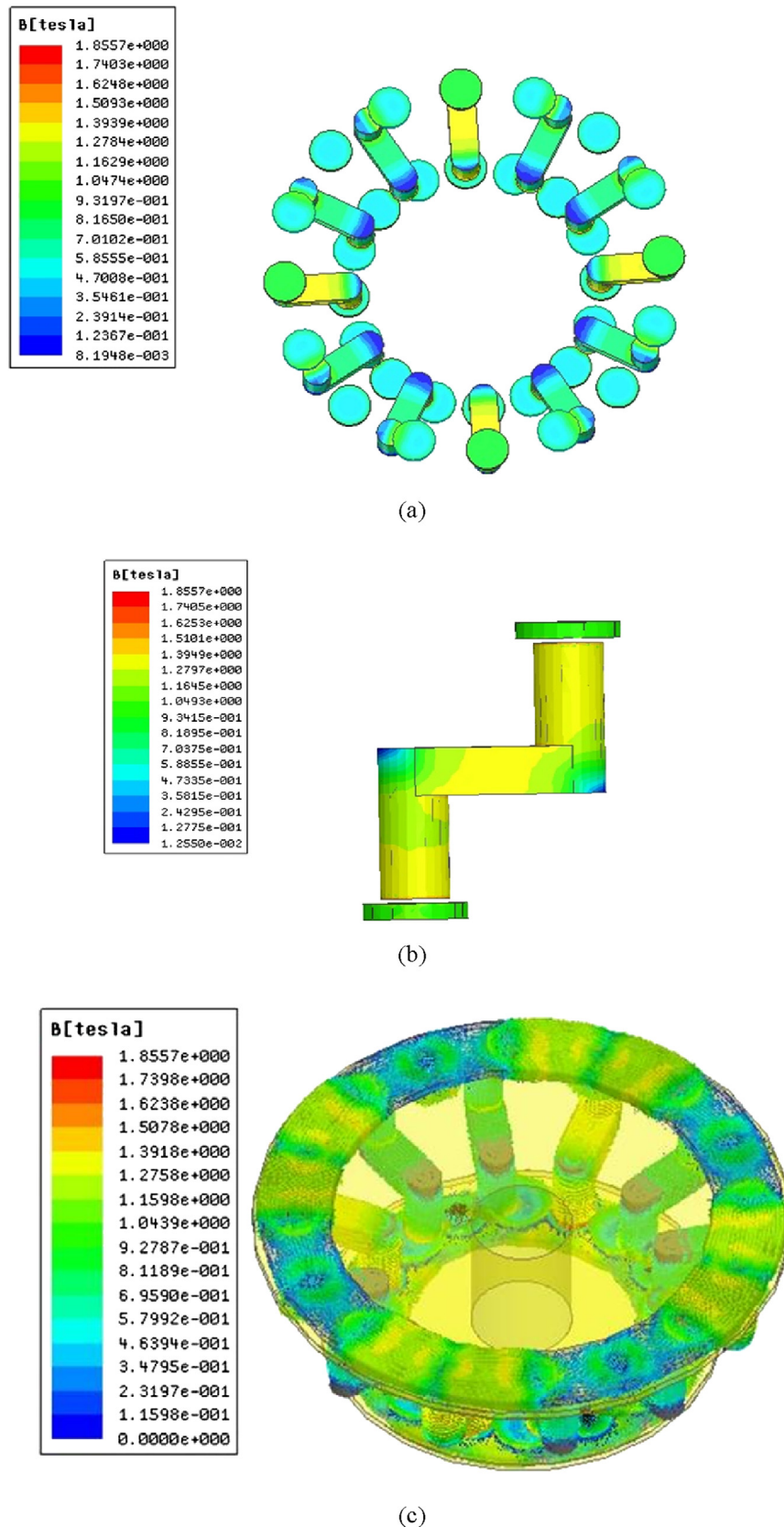


Fig. 5 – Magnetic flux densities of (a) overall machine (top view), (b) sample core and (c) overall machine in vector form.

drawback for the simulation time. Therefore an optimized value selection is important for the validity and reliability of the design. On the other hand, the ferromagnetic and

conducting parts of the units should take much attention in order to obtain an accurate simulation. The mesh types are considered as triangular and the meshes are applied intensely

for magnetic units such as core, back-iron, magnets and coil. The meshes have also been enhanced for edges and tips in order to achieve better simulation results. For the electrical connection of the windings in Fig. 3(a), the windings at the top and bottom tips of each core have been connected in series. For the overall phase connections we refer to Refs. [22–24].

A sample core consisting of 40 laminated layers with 0.5 mm thickness is shown in Fig. 4(a). In order to obtain a circular form, each layer has its specific width. The machine has 12 cores in total. It has been proven in our previous study that this core geometry enhances the cogging torque value of the machine [6,22]. At the tips of the cores, the coils are located.

The adjacent core tips and concentrated coils (with the distribution factor 1) are situated on the stator with an electrical angle of 22.5° . In the rotor unit shown in Fig. 4(b), the magnet housings are indicated on the yellow filling material. There exist 16 circular pair poles in the machine. Note that there exist also housings at the top rotor for the same magnet sizes. The magnets are adjusted as 30 mm in diameter and 5 mm in thickness in the design. In order to sustain maximal flux, the back-irons contacts the magnets at both sides.

Magnetostatic simulations of PMG

Magnetostatic simulations are important to identify the flux density for different orientations of the rotors and stator. Because of the core geometry and the structures of rotor and stator, the flux topology differs from the earlier machines. In

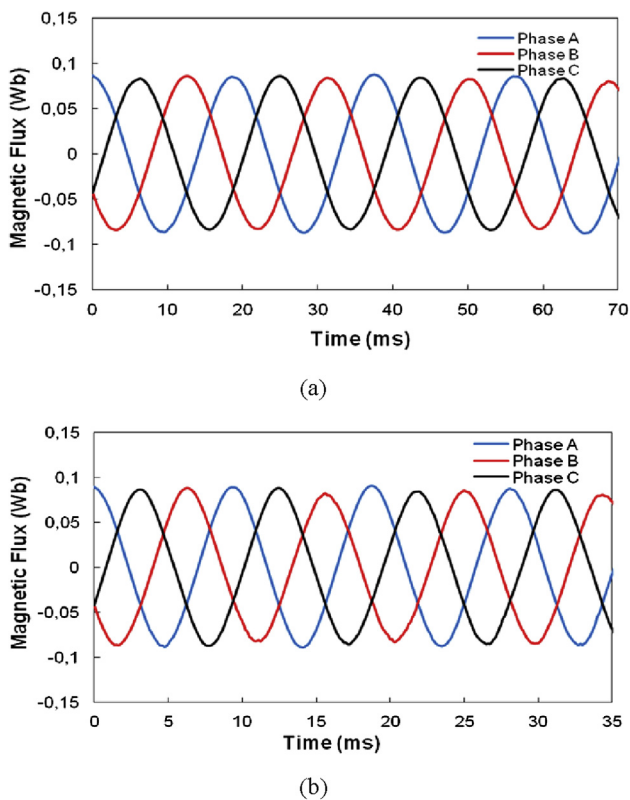


Fig. 6 – Magnetic fluxes passing from one coil at (a) 400 rpm and (b) 800 rpm.

Fig. 5(a), the flux densities of two rotors and the stator at the middle are shown. From top to bottom, Fig. 5(a) gives the minimal and maximal flux densities of 0.47 T and 1.3 T, respectively. Note that the flux densities become zero at the inner edges of cores. B becomes maximal in the core, when two magnets come nearby the core tips as usual. After each 22.5° , four magnets come to the same angular position with the cores. Therefore these regions have the maximal flux on the cores. In Fig. 5(b), the maximal B values are seen in detail. The edges at the middle part of the core has nearly zero density. This detailed figure also proves the validity of the core thickness, since the values do not exceed the B – H values in Fig. 2. Fig 5(c) shows the vectoral form of the field. This figure also includes the field pattern on the back-irons. The maximal field value is seen as 1.3 T in the back-iron.

Note that the field forms a closed circular form from one magnet to the adjacent ones by passing through the adjacent cores. Therefore there should be an optimal distance for the magnets while they are located at the lateral regions.

Magnetodynamic simulations of PMG

The transient solutions have been run during at least four periods. Fig. 6(a,b) presents a representative flux plot. The flux variations occur between ± 0.08 Wb. Note that the rotor speed only effects the time duration of the alternance change. While

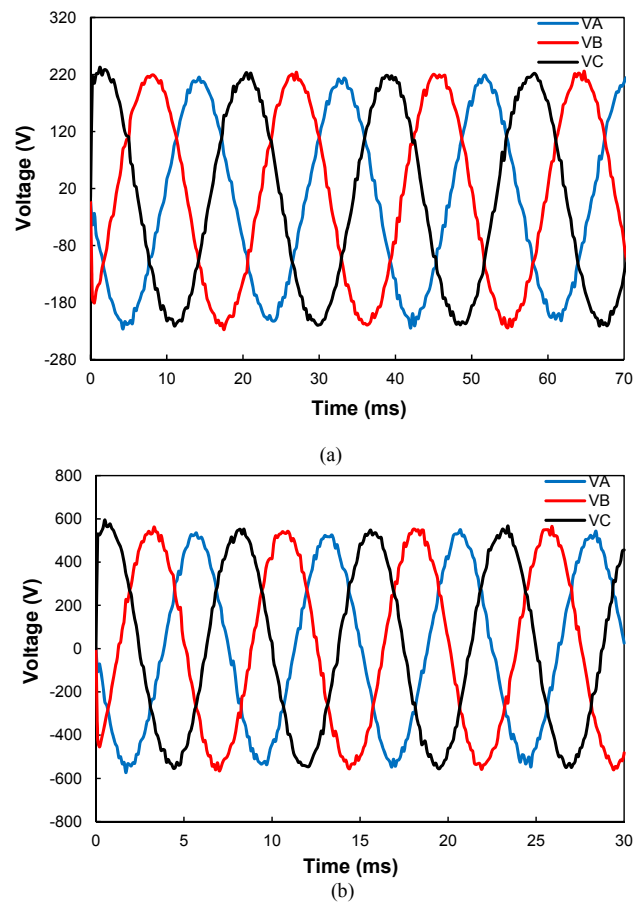


Fig. 7 – Phase voltages at the no-load case for (a) 400 rpm and (b) 1000 rpm.

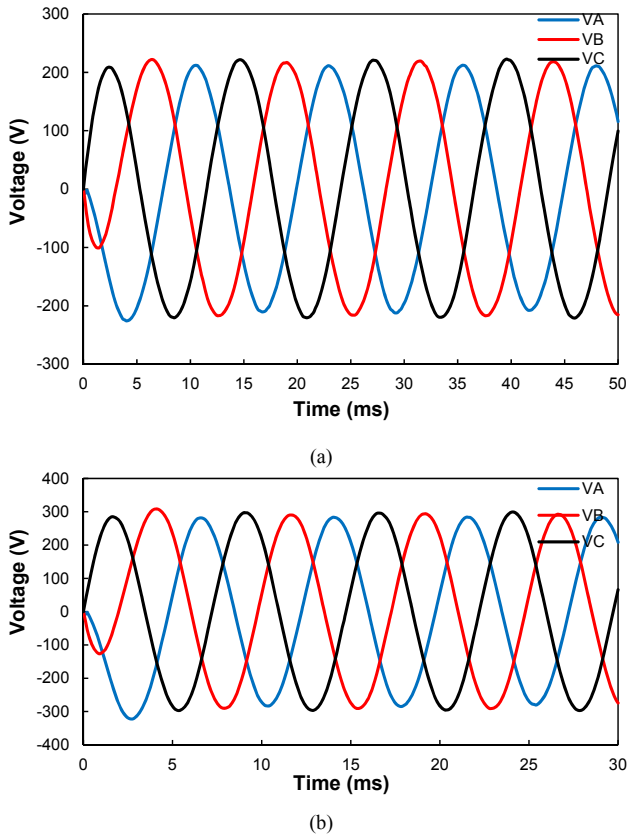


Fig. 8 – Phase voltages for 40 ohm load in the case of (a) 600 rpm and (b) 1000 rpm.

one period of the flux gets 10 ms for 800 rpm, it doubles for 400 rpm. Note also the flux phase shifts between three phases in accordance with the electrical angle.

There exists perfect symmetry in the flux waveforms, which confirm the accuracy of the flux topology. Due to the circular trajectory, the fluxes are obtained as sinusoidal waveforms. In another recent study of Kurt and Gor [23,24], the maximal magnetic flux of the machine without the back-iron has been found as 0.02 Wb, whereas in the recent machine 0.08 Wb has been obtained. Thus it is proven that the back-iron unit in the rotor is vital to increase the flux of the recent machine. Besides, the optimizations of the air gap value also assists to achieve that finding.

Fig. 7(a,b) shows sample waveforms from the transient simulation for the no-load case of the operation. Initially, it is obvious that the phases have correct phase shift with the same sinusoidal waveform. Indeed, the maximal amplitude of each phase is obtained with the phase shift of 120° as usual. There exist slight harmonicity due to the transient numerical analyzes, since the time evaluation has not been kept so short. At the rotor speed 400 rpm, the maximal peak to peak voltage is found as $V_{pp} = 222$ V.

Whereas the maximal value increases at 565 V for the rotor speed of 1000 rpm (Fig. 7(b)). Note that both of the plots have been obtained at the no-load case. In the case of electrical load (i.e. 40 Ω), the maximal voltage value is obtained as 222 V for 600 rpm (see in Fig. 8(a)). In the case of 1000 rpm, maximal amplitude decreases to 290 V for the same electrical load.

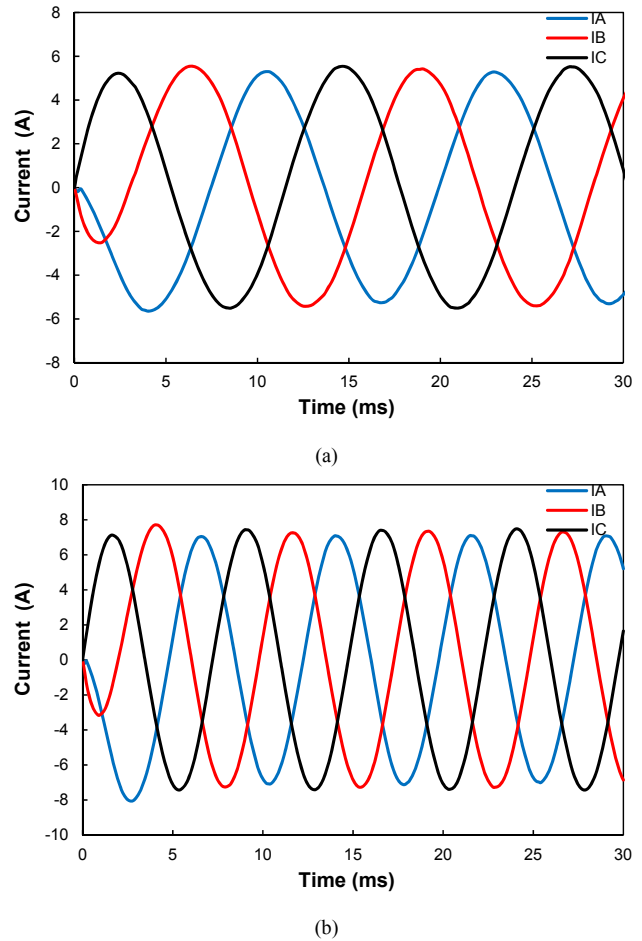


Fig. 9 – Phase currents for 40 ohm load in the case of (a) 600 rpm and (b) 1000 rpm.

Thus the load gets a certain potential from the initial stage. It is also interesting that the harmonics decay. In laboratory experiments performed by other machines, these kind of harmonicity annihilations were also observed before after the addition of the load.

In Fig. 9(a,b), the current waveforms are shown. These values give the phase current which is determined in the same

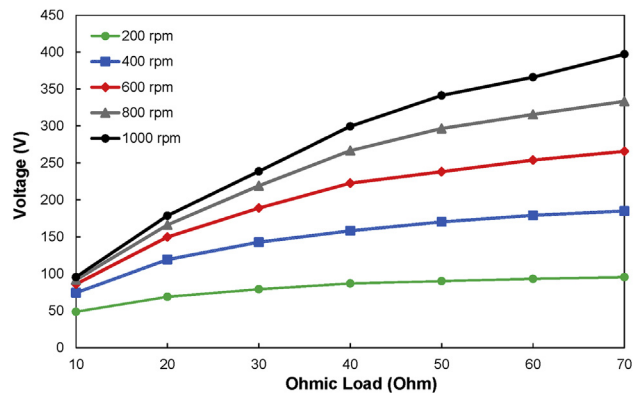


Fig. 10 – Voltage vs. ohmic load for different rotor speeds.

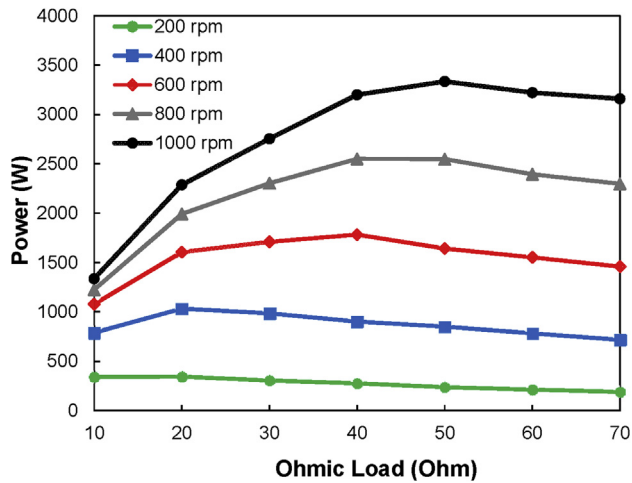


Fig. 11 – Power vs. ohmic load at different speeds.

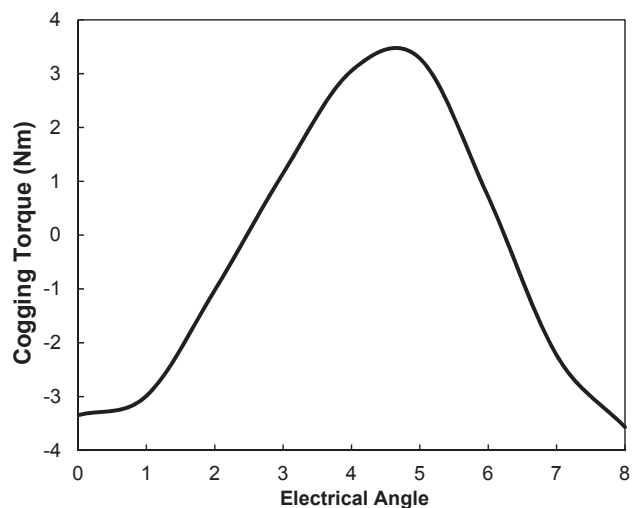


Fig. 12 – Cogging torque variation vs. electrical angle.

connection configuration in Refs. [23,24]. After one period, the effect of the initial value reaches its stationary response and ideal currents are obtained. While the maximal currents are found as 5.5 A for 600 rpm, it becomes 7.4 A for 1000 rpm. Perfect sinusoidal is obtained for the current. This proves that the machine design is stable for each phase.

Note that these currents flow from two adjacent coils located at the tips of the core. The phase shifts among the phases are perfect. The connection of the windings can be done in different ways in order to increase the current for each phase, since the generator has 24 coils.

Table 2 – THD values for various electrical loads at 1000 rpm.

Ohmic load (Ohm)	THD (%)
50	3.4
40	3.4
30	3.2
20	3.1
10	2.9

Simulations have been carried out for different electrical loads as seen in Fig. 10. According to the transient simulations, the maximal amplitudes increase upto $V = 341$ V at the load 50Ω for 1000 rpm. Indeed, the maximal voltage can be expected for slightly high loads. When the rotor speed increases, linearly the output voltage increases. However, the maximal amplitude becomes 100 V and it does not change for the rotor speed 200 rpm for each loads. While the speed decreases, the increment rate of the amplitude also decreases smoothly as also seen in previous experiments with other generators. When the load is adjusted as 70Ω , the voltage values increase further upto 397 V for 1000 rpm. Note also that the voltages for other speeds also increase at that load.

Fig. 11 gives the output power estimation for different ohmic loads in terms of different rotor speeds. Note that it is the power of three phases. While the rated power is obtained around 50Ω for 1000 rpm, the maximal power gets to lower loads such as 20Ω and 10Ω for lower rotor speeds as usual.

The detailed simulations indicate that the power of 3.4 kW is available from the generator at 1000 rpm. The power density of the machine become $P_v = 336 \text{ kW/m}^3$, which is a good value for axial generators according to the literature if the power densities are considered between 6 kW/m^3 and 700 kW/m^3 [11].

Finally, the result of the cogging torque is given in Fig. 12. The net cogging torque value fluctuates between ± 5.6 Nm. Comparing the previous studies [6,21], it is a good value for an axial generator with cores and back irons. Since the flux increases at the vicinity of core tips, it produces a net torque. Note also that the new shaped core also assists to decrease the torque in that regard.

The machine has good total harmonic distortion (THD) values, when several resistive loads have been attached to the output of the phases. Table 2 shows the THD values for various loads at 1000 rpm.

It is obvious that the THD values do not exceed 3.4% and it is convenient for a new machine.

Conclusions

The electromagnetic design and 3D simulation of a new permanent magnet generator have been carried out. The new machine has an innovative flux topology with 16 rare earth permanent magnet and 24 windings with a specific laminated core structure and back-irons in two rotors. The maximal flux densities are estimated as 1.3 T inside the core for 1.5 mm air gap. The machine has good sinusoidal voltage waveform. This is also valid for magnetic flux and current waveforms. According to the simulations for different rotor speeds, the rated power is found as $P = 3.4 \text{ kW}$ for 1000 rpm around 50Ω . Thus it corresponds to the power density of $P_v = 336 \text{ kW/m}^3$ as a good power density value. The maximal cogging torque value is measured as 3.6 Nm, which is a promising value for an axial machine with cores and back-irons. Consequently, the new designed machine can be used for the household wind energy applications due to its basic production, sinusoidal output and good power density values. The sinusoidal wave shapes and their THD values are also promising for the preliminary studies.

Acknowledgements

The authors are grateful to Gazi University, Scientific Researches Project Unit for the support of this project under the Grant No: 07/2011-25 and EU Ministry of Turkey National Agency Grant No: 2015-1-TR01-KA203-021342 (Innovative European Studies on Renewable Energy Systems) for the compilation of the research. This machine has been suggested to TPE as a new patent under No. 2014/16384.

REFERENCES

- [1] Kurt E, Aslan S, Demirtas M, Güven ME. Design and analysis of an axial-field permanent magnet generator with multiple stators and rotors. In: Proceedings of the 2011 3th. IEEE Conf. power Engineering, energy and electrical Drives, Torremolinos (Malaga), Spain; 2011. p. 2–4.
- [2] Yıldız E, Aydemir MT. Analysis, design and implementation of an axial flux, permanent magnet machine to be used in a low power wind generator. *J Fac Eng Archit Gazi Univ* 2009;24(3):525–31.
- [3] Singh BP, Dwivedi S. A state of art on different configurations of permanent magnet brushless machines. *IE (I) J-EL* 2006;78:63–73.
- [4] Barave SP, Chowdhury BH. Optimal design of induction generators for space applications. *IEEE Trans Aerosp Electron Sys* 2009;45(3):1126–37.
- [5] Guannan D, Haifeng W, Hui G, Guobiao G. Direct drive permanent magnet wind generator design and electromagnetic field finite element analysis. *IEEE Tran Appl Supercond* 2010;20(3):1883–7.
- [6] Kurt E, Gör H, Demirtaş M. Theoretical and experimental analyses of a single phase permanent magnet generator (PMG) with multiple cores having axial and radial directed fluxes. *Energy Convers Manag* 2014;7:163–72.
- [7] Wallace RR, Lipo TA, Moran LA, Tapiai JA. Design and construction of a permanent magnet axial flux synchronous generator. Milwaukee: Electric Machines and Drives Conference IEEE; 1997. MA1/4.1–MA1/4.3.
- [8] Bumby JR, Martin R. Axial-flux permanent-magnet air-cored generator for small-scale wind turbines. *Proc IEE- Electr Power Appl* 2006;152(5):63–73.
- [9] Qamaruzzaman A, Pradipta P, Dahono A. Analytical prediction of inductances of slotless axial-flux permanent magnet synchronous generator using Quasi-3D method. *Int J Electr Eng Inf* 2009;1(2):115–25.
- [10] Vansompel H, Sergeant P, Dupre L. Optimized design considering the mass influence of an axial flux permanent-magnet synchronous generator with concentrated pole windings. *Magn IEEE Trans* 2010;46(12):4101–7.
- [11] Gholomian SA, Yousefi A. Power density comparison for three phase non-slotted double-sided AFPM motors. *Aust J Basic Sci* 2010;4(12):5497–955.
- [12] Sadeghierad M, Lesani H, Monsef H, Darabi A. Design considerations of high speed axial flux permanent magnet generator with coreless stator. Singapore: Power Engineering Conference, IPEC 2007; 2007. p. 1097–102.
- [13] Muljadi E, Butterfield CP, Wan UH. Axial-flux modular permanent-magnet generator with a toroidal winding for wind-turbine applications. *IEEE Trans Ind Appl* 1999;35(4):831–6.
- [14] Li J, Choi DW, Cho YH. Development of a natural cooled axial flux permanent magnet generator for wind turbine. Hangzhou: Industrial Electronics (ISIE), 2012 IEEE International Symposium; 2012. p. 635–40.
- [15] Javadi S, Mirsalim M. A coreless axial-flux permanent-magnet generator for automotive applications. *IEEE Trans Magn* 2008;44(12):4591–8.
- [16] Dosiek L, Pillay P. Cogging torque reduction in permanent magnet machines. *Ind Appl IEEE Trans* 2007;43(6):1565–71.
- [17] Chan TF, Weimin W, Lai LL. Magnetic field in a transverse- and axial-flux permanent magnet synchronous generator from 3-D FEA. *Magn IEEE Trans* 2012;48(2):1055–8.
- [18] Bumby JR, Martin R. Axial flux permanent magnet generator for engine integration. In: Published at the 12. Int. Stirling Engine Conf., Durham; 2005.
- [19] Chan CC. Axial-field electrical machines-design and applications. *IEEE Trans Energy Conv* 1987;2(2):294–300.
- [20] Vansompel H, Sergeant P, Dupre L, Van den Bossche A. Axial-flux PM machines with variable air gap. *Ind Electron IEEE Trans* 2014;61(2):730–7.
- [21] Rasekh Alireza, Sergeant Peter, Vierendeels Jan. Convective heat transfer prediction in disk-type electrical machines. *Appl Therm Eng* 2015;91:778–90.
- [22] Kurt E, Aslan S, Gör H, Demirtaş M. Electromagnetic analyses of two axial-flux permanent magnet generators (PMGs). Istanbul, Turkey: Power Engineering, Energy and Electrical Drives (POWERENG), 2013 Fourth International Conference IEEE; 2013. p. 290–4.
- [23] Gor H, Kurt E. Waveform characteristics and losses of a new double sided axial and radial flux generator. *Int J Hydrogen Energy* 2016. <http://dx.doi.org/10.1016/j.ijhydene.2015.12.172>.
- [24] Gor H, Kurt E. Preliminary studies of a new permanent magnet generator (PMG) with the axial and radial flux morphology. *Int J Hydrogen Energy* 2016;41(17):7005–18.